Hindawi
International Journal of Polymer Science
Volume 2019, Article ID 4737384, 11 pages
https://doi.org/10.1155/2019/4737384

Research Article

Experimental Investigation on Mechanical Properties of Hybrid Steel and Polyethylene Fiber-Reinforced No-Slump High-Strength Concrete

Tian-Feng Yuan,[1] Jin-Young Lee,[2] Kyung-Hwan Min,[3] and Young-Soo Yoon[1]

[1]*School of Civil, Environmental and Architectural Engineering, Korea University, 145 Anam-ro, Seongbuk-gu, Seoul 02841, Republic of Korea*
[2]*Department of Civil Engineering and Applied Mechanics, McGill University, 817 Sherbrooke Street West, Montreal, Quebec, Canada H3A0C3*
[3]*Rail Research Institute, Chungnam National University, 99 Daehak-ro Yuseong-gu, Daejeon 34134, Republic of Korea*

Correspondence should be addressed to Young-Soo Yoon; ysyoon@korea.ac.kr

Received 4 April 2018; Accepted 29 January 2019; Published 20 March 2019

Guest Editor: Aamer Bhutta

This paper presents experimental investigations on the mechanical properties of no-slump high-strength concrete (NSHSC), such as the compressive and flexural strength. First, to determine the proper NSHSC mixtures, the compressive and flexural strength of three different water-to-binder ratios (w/b) of specimens with and without polyethylene (PE) fiber was tested at test ages. Then, the effect of hybrid combinations of PE fiber and steel fiber (SF) on the compressive strength, flexural strength, flexural toughness, and flexural energy dissipation capacity was experimentally investigated. Furthermore, the various hybrid fiber-reinforced NSHSCs were evaluated, and their synergy was calculated, after deriving the benefits from each of the individual fibers to exhibit a synergetic response. The test results indicate that a w/b of 16.8% with or without fibers had lower strength and flexural strength (toughness) than those of other mixtures (w/b of 16.4% and 17.2%). Specimens with a hybrid of SF and short PE fibers exhibited a higher compressive and flexural strength, flexural toughness, energy dissipation capacity, and fiber synergy in all considered instances.

1. Introduction

No-slump concrete, also known as zero-slump concrete, is defined as concrete with 0-25 mm slump by the American Concrete Institute (ACI 211.3) [1]. It is widely used for the production of paving blocks, masonry blocks, concrete slabs, and prestressed concrete (PC) elements. To achieve adequate internal cohesion of the granular matrix, the water-to-binder ratio (w/b) must be low [2, 3]. The inclusion of the properties of self-compacting concrete (SCC) in no-slump to create self-compacting no-slump concrete (SCNSC) has been widely researched [4]. There are cases of no-slump concrete fabricated and used in structures, such as a no-slump mixture used at Alpe Gere dam in Italy and at Manicougan-I in Canada with the aid of large internal vibrators mounted on backhoes or bulldozers [3, 5]. However, all of those no-slump concrete mixtures are low or normal-strength concrete (20-60 MPa) and do not exceed 100 MPa of compressive strength. There has also been a lack of research on no-slump high-strength concrete with a compressive strength of over 120 MPa at 28 days.

The design method of no-slump high-strength concrete was based on that of ultra-high-performance cementitious materials, which have a very low water-to-binder ratio and can achieve good mechanical properties through controlling the packing density of the solid. However, cementitious composites are brittle, with a low tensile strength (flexural strength) and strain capacity. Hence, reinforcing concrete with randomly discontinuous fibers can improve ductility, toughness, and resistance to crack growth, and two or more types of fibers can be included to exploit their complementary and maximize the improvement [6]. Most of the

conventional fiber-reinforced cementitious materials involve the use of individual fiber types or hybrid single fiber types with different sizes. The individual fiber reinforcement method is effective in an only limited range of strain and crack opening and improved strength or ductility [7]. To improve strength and ductility, hybrid single fiber types with different sizes are generally used for ultra-high-performance cementitious materials [8, 9]. The hybrid fiber-reinforced composites have benefited from each of the individual fibers and exhibit a synergetic response. The various methods of hybridization include hybrids with different aspect ratios (lengths, diameters) and fiber types (tensile strength, modulus). The hybrid based on fiber aspect ratios results in a higher strength and improved fracture toughness of the composites, which control their microcracks and macrocracks, respectively. Hybrids based on fiber types use different properties of flexibility, in which a stiffer fiber provides the strength (first-crack strength, postcrack strength) and the other improves the toughness and strain capacity [10–14].

To date, there has been a lack of research on the combination of different fiber hybridizations in no-slump high-strength concrete. In this study, in order to filter out the effects on compressive strength, three different water-to-binder ratio (w/b) values with a fiber volume fraction of 0.0%, and 1.5% were fabricated and evaluated. In order to improve the tensile strength and strain capacity of NSHSC, the mixtures are hybrid polyethylene (PE) fibers and/or steel fibers (SF), and the compressive strength and flexural strength at test ages were evaluated. Additionally, the flexural toughness and the synergy of hybridization were evaluated. Therefore, this study is provided and used as a basic data to fiber-reinforced no-slump high-strength concrete.

2. Experimental Program

In this study, concrete with three values of water-to-binder ratios was prepared using no-slump high-strength concrete (NSHSC) hybrid polyethylene or/and steel fibers. The variable specimens were used with a fiber volume fraction of 0.0%, and 1.5%, with which two different lengths or types of fibers for suitable hybridization (0.0, 0.5, and 1.0) were adopted. All the variable specimens were tested for compressive strength according to test ages and flexural strength under four-point flexural loads. Furthermore, the absorbed flexure energy and synergy in the flexure of NSHSC by adding hybrid fibers were investigated. The detailed mixture proportions, materials, and mechanical test setup performed in this study are as follows.

2.1. Mixture Proportions and Materials. The cementitious materials of NSHSC in this study were Type I Portland cement (specific surface area of 3,492 cm^2/g, density of 3.15 g/cm^3) and silica fume produced in Norway (specific surface area of 200,000 cm^2/g, density of 2.20 g/cm^3). The sand grain size was smaller than 0.5 mm, and 10 μm diameter filler (specific surface area of 2.65 cm^2/g, density of 0.75 g/cm^3) including 99% SiO_2 was used in the mixture. To provide suitable workability, liquid polycarboxylate superplasticizer (SP) was used. Three different water-to-binder ratio (w/b) values and two different fiber lengths and types with several volume fractions were adopted in the mixture, as described in Tables 1 and 2. Table 3 shows the chemical and physical properties of these materials. The high-strength polyethylene fibers and high-strength straight steel fibers were used to prevent fiber fracture before the fiber slip occurred between the fiber and the matrix. Two different lengths of PE fibers were adopted, and the fiber exhibited the following characteristics: an equivalent diameter of 31 μm, a length of 12 or 18 mm, and a nominal tensile strength of 2,900 MPa. The SF used had an equivalent diameter of 0.2 mm, a length of 19.5 mm, and a nominal tensile strength of 2,650 MPa. The physical and geometric properties of the fibers are separately listed in Table 4. All variable specimens were designed based on the relative density method [15] and mixing procedure as shown in Figure 1. Furthermore, the specimens were cured after casting and demolding for 24 hours in a room with steady temperature and humidity until the testing date (28 days), at a temperature of 20 ± 1°C and a relative humidity of 60 ± 5%.

Table 1: The proportion of materials in the NSHSC mixture by cement weight ratio.

Cement	Silica fume	Filler	Sand	Water	Fiber	w/b
1.00	0.25	0.30	1.10	0.20-0.22	Table 2	

2.2. Details of the Mechanical Test and Setup

2.2.1. Slump and Compressive Strength Test. The slump tests were carried out according to ASTM C1437 [16]. Each variable specimen was tested after adding SP to obtain the target slump which was 0 mm of slump according to trial and error (Figure 1), then compacted by the exertion of pressure after pouring the concrete into test molds, and surface finishing was performed. This method is according to the previously published researches [17, 18], the use of a modified steel plate to compact the concrete into molds to produce specimens of the same density.

The compressive strength tests were carried out according to ASTM C39 [19], and the test setup is shown in Figure 2(a). Six cylindrical specimens for each variable were fabricated and used in the compressive strength tests. The cylindrical specimens with a diameter of 100 mm and height of 200 mm were used and tested at 7 and 28 days after casting. The test used a universal testing machine (UTM) with a maximum capacity of 250 tons under the monotonic rate of 0.2 mm/min.

2.2.2. Flexural Strength Test. Three prismatic specimens for each variable were fabricated and tested under four-point flexure according to ASTM C1609 [20]. The prismatic specimens used for measuring flexural strength had a width of 100 mm, height of 100 mm, and length of 400 mm. Each prism specimen was turned 90° from the casting surface and then failed completely at midspan. To eliminate the midspan deflection capacity of the prismatic specimens, a specialized steel frame with two linearly variable differential transformers (LVDTs) were attached to the side of the

Table 2: Details of various w/b of specimens and fiber hybridization.

	w/b (%)	w/c (%)	PE fibers (12 mm/%)	PE fibers (18 mm/%)	Steel fibers (19.5 mm/%)
U16.4-NF	16.4	0.20	—	—	—
U16.8-NF	16.8	0.21	—	—	—
U17.2-NF	17.2	0.22	—	—	—
U16.4-18PE1.5	16.4	0.20	—	1.5	—
U16.8-18PE1.5	16.8	0.21	—	1.5	—
U17.2-18PE1.5	17.2	0.22	—	1.5	—
U16.4-PP1.5	16.4	0.20	0.5	1.0	—
U17.2-PP1.5	17.2	0.22	0.5	1.0	—
U16.4-12SP0.5	16.4	0.20	0.5	—	1.0
U17.2-12SP0.5	17.2	0.22	0.5	—	1.0
U16.4-18SP1.0	16.4	0.20	—	1.0	0.5
U17.2-18SP1.0	17.2	0.22	—	1.0	0.5

Table 3: Chemical compositions and physical properties of cementitious materials.

	Surface area (cm^2/g)	Density (g/cm^3)	Chemical composition (%)							
			SiO_2	Al_2O_3	Fe_2O_3	CaO	MgO	SO_3	Na_2O	K_2O
Cement	3,492	3.15	21.16	4.65	3.14	62.79	2.81	2.13	—	—
Silica fume	200,000	2.20	96.00	0.25	0.12	0.38	0.10	<0.2	—	—
Filler	2.65	0.75	99.60	0.31	0.025	0.010	0.006	—	0.009	0.004

Table 4: Properties of polyethylene and steel fiber.

	Diameter, d_f	Length, l_f (mm)	Aspect ratio (l_f/d_f)	Density (g/cm^3)	Tensile strength (MPa)	Elastic modulus (GPa)
Polyethylene fiber	31 μm	12	387	0.97	2,900	100
		18	580			
Steel fiber	0.2 mm	19.5	97.5	7.8	2,650	200

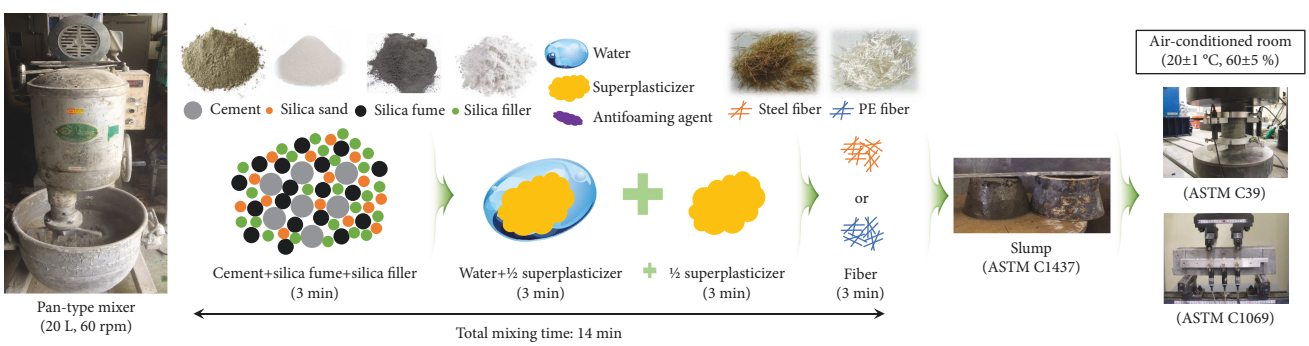

Figure 1: Mixing, curing, and test method of NSHSC.

prismatic specimens. The tests were performed using the UTM described above, switched to displacement control at a rate of 0.3 mm/min (Figure 2(b)). The curing conditions were the same as those of the cylindrical specimens in the compressive strength test.

According to ASTM C1609, a load versus deflection curve was obtained, which can be calculated based on different toughness indices I_5, I_{10}, and I_{30}. The toughness index defined by ASTM C1018 [21] is calculated from the area under the flexural load-deflection curve up to a given deflection divided by the first cracking in the area under the same curve. Furthermore, the energy absorbed and toughness factor of the various fiber-reinforced specimens can be further analyzed. The calculation method for the flexural

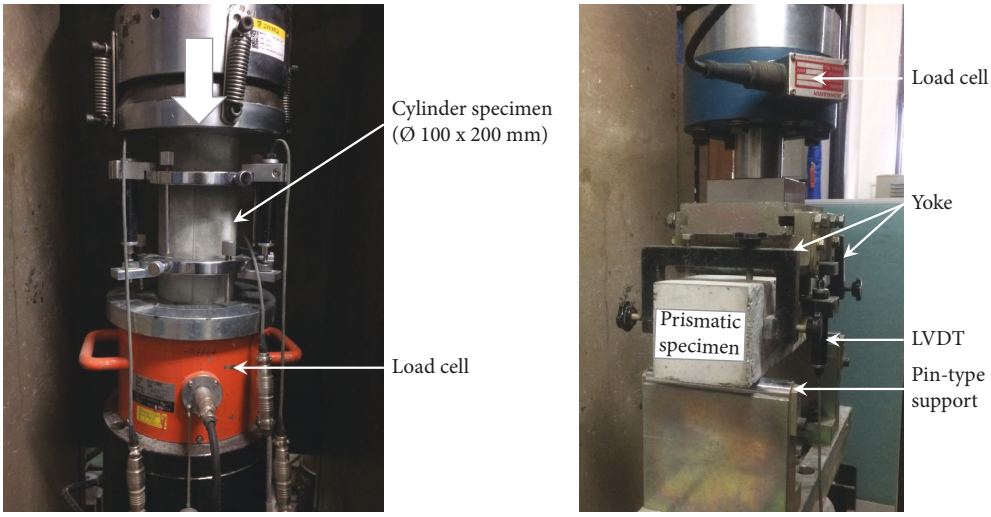

(a) (b)

Figure 2: Mechanical test setup: (a) compressive test (ASTM C39) and (b) flexural test (ASTM C1609).

Table 5: Test results of compressive and flexural strength.

	Compressive strength										Flexural strength							
	7 days (MPa)					28 days (MPa)					28 days (MPa)					Toughness index		
	Mean	COV	Test results			Mean	COV	Test results			Mean	COV	Test results			I_5	I_{10}	I_{30}
U16.4-NF	90.9	4.0%	92.9	85.9	94.1	120.9	4.3%	126.8	114.3	121.5	6.0	29.0%	8.3	5.6	4.1	—	—	—
U16.8-NF	89.1	2.3%	90.9	86.2	90.2	109.1	2.3%	109.2	105.9	112.1	3.6	18.6%	4.3	3.7	2.7	—	—	—
U17.2-NF	91.9	0.6%	92.1	91.2	92.4	122.0	1.8%	125.0	119.7	121.3	5.7	15.7%	5.3	4.9	6.9	—	—	—
U16.4-18PE1.5	80.9	4.7%	80.3	76.6	85.7	121.9	4.5%	120.1	129.4	116.2	15.3	4.0%	15.8	15.5	14.4	4.9	11.0	43.3
U16.8-18PE1.5	79.0	4.2%	83.3	75.2	78.5	120.8	3.1%	125.0	116.0	121.4	15.2	15.4%	18.2	14.7	12.6	5.2	11.2	41.9
U17.2-18PE1.5	81.0	1.5%	82.3	81.3	79.4	124.9	0.1%	125.0	124.7	125.0	23.1	19.3%	23.1	28.6	17.7	5.3	12.2	62.2
U16.4-PP1.5	81.2	1.7%	80.9	79.7	83.1	116.2	3.1%	118.9	111.1	118.4	19.6	17.0%	13.4	20.5	16.8	4.9	10.4	32.4
U17.2-PP1.5	81.9	1.6%	80.2	83.3	82.1	117.3	1.6%	119.5	117.2	115.0	22.1	11.6%	19.2	24.3	22.8	5.5	11.8	48.4
U16.4-12SP0.5	86.0	3.9%	82.5	85.0	90.6	123.2	0.7%	122.9	124.5	122.3	19.0	8.6%	20.3	28.1	19.5	5.5	17.1	71.1
U17.2-12SP0.5	86.3	5.0%	82.6	92.3	84.0	123.4	0.3%	123.9	123.1	123.1	21.9	8.5%	24.1	19.6	22.1	5.4	12.2	58.8
U16.4-18SP1.0	85.9	1.5%	80.9	79.7	83.1	123.3	0.7%	122.0	123.9	123.9	14.7	5.1%	13.9	14.3	15.8	4.8	11.2	51.5
U17.2-18SP1.0	86.0	1.6%	80.2	83.3	82.1	122.9	3.5%	128.4	122.2	118.1	18.5	10.5%	21.0	18.3	16.3	5.3	15.7	59.3

Note: mean = mean value of test strength; COV = coefficient of variation.

toughness factor (FT_δ) was defined by the Japan Society of Civil Engineers (JSCE) [22] and the details of the equation is as follows:

$$FT_\delta = \frac{T_{b,\delta} L}{\delta b d^2}, \quad (1)$$

where $T_{b,\delta}$ denotes the area under the curve to a flexural specimen displacement of δ, L denotes the span of the specimen, and b and d denote the width and depth of the specimen.

3. Experimental Results and Discussion

3.1. Compressive Strength. Table 5 summarizes the average strength and coefficient of variation at test ages based on the compressive strength test. A minimum of three concrete cylinders were prepared and tested at 7 and 28 days after curing conditions.

The NSHSC specimen with a w/b of 17.2% and without fibers had slightly higher compressive strength with a small coefficient of variation among the specimens. The exhibited values of compressive strength (and coefficient of variation) were 91.9 (0.6%) and 122.0 (1.80%) MPa at 7 and 28 days, respectively. The NSHSC specimens with a fiber volume fraction of 1.5% of 18 mm PE fibers showed similar behavior and strength at 28 days to NSHSC without fibers, and specimen U17.2-18PE1.5 demonstrated a slightly high strength with a small value of the coefficient of variation as well. Furthermore, the addition of PE fibers improved the energy dissipation capacity, which inhibits crack propagation and development in the concrete matrix, and ensured that the

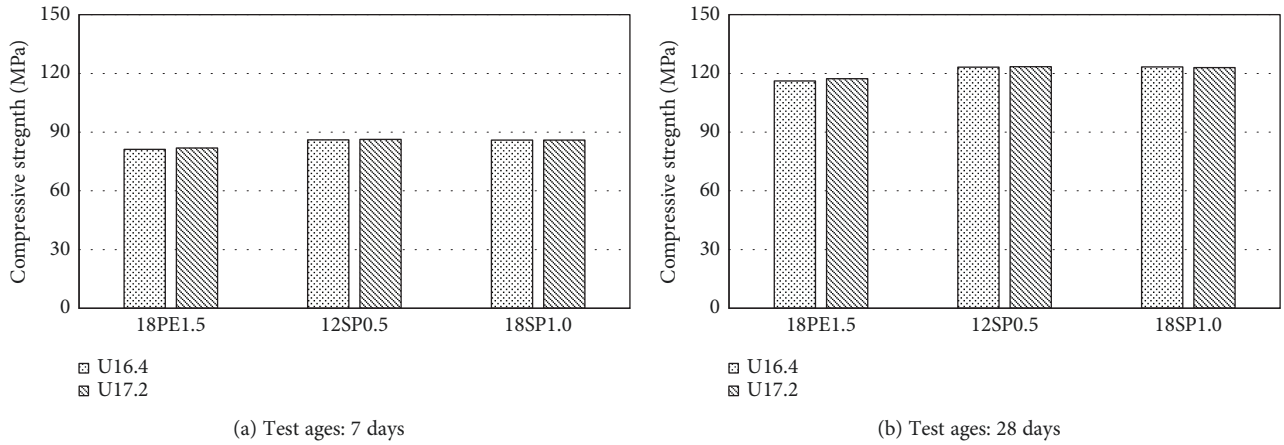

Figure 3: Compressive strength of hybrid fibers reinforced NSHSC.

PE fiber-reinforced specimens were not completely crushed [23]. A w/b of 16.8% with or without fibers resulted in low-strength behavior; hence, it was eliminated from the evaluation of the mechanical performance of fiber hybridization.

The compressive properties of hybrid PE fibers and SF-reinforced NSHSC at 7 and 28 days are shown in Figure 3. The specimens included PE fibers with an aspect ratio of 387 and 580 (U16.4-PP1.5, U17.2-PP1.5), respectively, and exhibited low compressive strength, approximately 4.8-6.1% lower than that of specimens with different fiber types. The specimens with different lengths of the PE fibers and SF were found to have similar compressive strengths of over 85 and 123 MPa at 7 and 28 days, respectively.

3.2. Flexural Properties of Specimens with Combined Fibers

3.2.1. Flexural Behavior. In the flexural strength test, the specimens without PE fibers had a sudden load drop immediately after the first crack occurred. This means that the values of the first-cracking strength and postcracking strength were the same in the specimens without fibers, as the load-carrying capacity of those specimens decreased to almost zero immediately after matrix cracking. Specimen U16.8-NF exhibited lower flexural strength, in a manner similar to compressive strength. Because of the fiber bridging with the matrix and the propagation of cracks in the loading process, specimens reinforced by 1.5 vol.% of PE fibers (18 mm) were found to have an increased load-carrying capacity after matrix cracking, which was approximately 1.5-3.1 times the postcracking strength of the specimens without fibers. Otherwise, midspan deflection increased continuously during the loading the process, and eventually, a localized crack occurred due to the sharply decreasing load in the prismatic specimens. Of those, specimen U17.2-18PE1.5 showed the most enhanced postcracking strength among the specimens with PE fibers.

Based on the load-deflection curve, the different toughness indices I_5, I_{10}, and I_{30} of the fiber-reinforced NSHSC specimens were calculated. Specimens with w/b of 16.4% and 16.8% using 1.5 vol.% of PE fibers had similar toughness indices values at the same deflection. Toughness index values as high as 62.2 were measured with a w/b of 17.2% containing 1.5 vol.% PE fibers. According to recent studies [24], the fiber-reinforced cementitious composites with toughness indices $I_5 > 5$, $I_{10} > 10$, and $I_{30} > 30$ can be defined as strain-hardening composites. Specimens with PE fibers studied in this investigation were based on the above criteria and can, therefore, be defined as strain-hardening materials, as shown in Table 5. In addition, NSHSC with 1.5 vol.% PE fibers exhibited high ductility along with high toughness indices; thus, the average midspan deflection was over 6 mm, which was about 2% of the specimen's span length. This is because the PE fibers induced a delay in localized cracking and ensured the formation of multiple cracks due to the increased energy absorption capacity [25].

3.2.2. Flexural Behavior of Hybrid Fiber-Reinforced NSHSC. Figure 4 shows the flexural load versus midspan deflection curve of hybrid fiber-reinforced NSHSC. Because the combination of two or more fibers provides different responses to the cracking process during different stages of loading, the flexural strength was increased by specimens containing a composite with hybrid fibers, rather than single fiber reinforcement. Moreover, all of the specimens show strain-hardening behavior based on the above criteria, and the values are noted in Table 5. The hybrid PE fibers with different lengths (U16.4-PP1.5, U17.2-PP1.5) exhibited a somewhat low flexural strength but similar strain capacities (high strain capacities) to those of the specimens with hybrid PE fibers and SF. This is due to the low modulus of the PE fibers, which leads to low strength and the high strain capacity, and the high strength is due to the high modulus of the SF [26, 27]. Furthermore, in the hybrid SF and PE fiber specimens, the hybrid method with long SF and short PE fibers exhibited higher flexural strength, toughness, and strain capacity than those of the combined long SF and long PE fibers (Figure 4). For example, specimen U16.4-12SP0.5 exhibited a high postcracking strength and toughness index at 15.5δ, which were approximately 29.3%, and 37.9% higher than those of specimen U16.4-18SP1.0, respectively. In terms of the different sizes of the fibers, the short fibers bridge microcracks and control their coalescence into macrocracks, whereas the long fibers

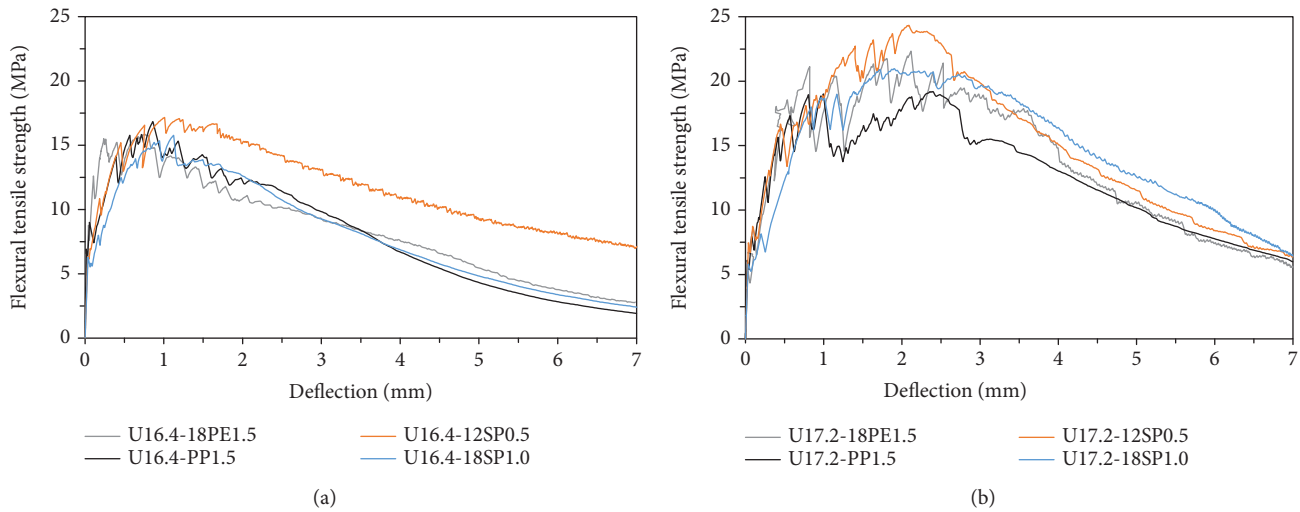

Figure 4: Flexural load-deflection curves: (a) w/b of 16.4% and (b) w/b of 17.2%.

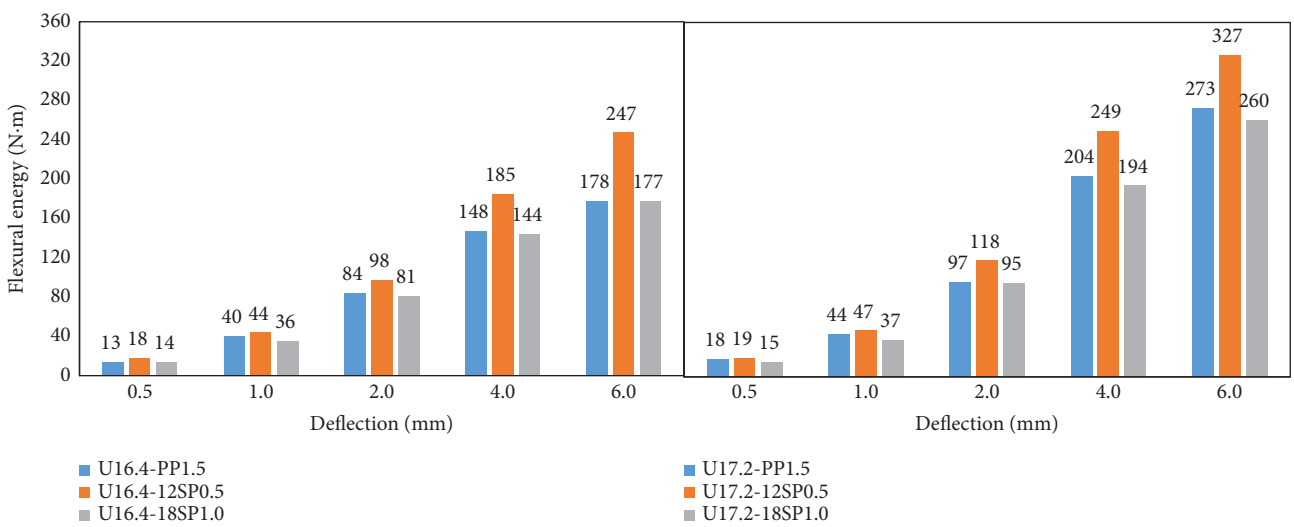

Figure 5: Flexural energy absorption values calculated according to the curve in Figure 4.

contribute to arrest and prohibit the propagation of macrocracks [28, 29]. Hence, specimens achieved high strength, toughness, and strain capacity according to the control of micro- and macrocracks.

The flexural strength versus w/b of hybrid fiber-reinforced NSHSC is shown in Figure 4 and Table 5. Specimens with w/b of 17.2% and hybridization fibers PP1.5, 12SP0.5, and 18SP1.0 had the average postcracking strength of 22, 22, and 19 MPa, respectively. These values are approximately 29.4%, 15.8%, and 58.3% higher than specimens with a w/b of 16.4% and hybridization fibers, respectively. However, specimens with a w/b of 16.4% and hybridization fibers exhibited high toughness and over 2% of the specimen's span length in the deflection. Because specimen U17.2 had slightly higher compressive strength than specimen U16.4, the postcracking strength increased with the increasing interfacial bond strength between the fiber and the matrix and was strongly influenced by the fiber orientation and dispersion in the specimens [30, 31].

3.2.3. Flexural Energy Absorption and Toughness Factor. The energy absorption was calculated for flexural deflections of 0.5, 1.0, 2.0, 4.0, and 6.0 mm in order to evaluate the effect of fiber hybridization, especially for the energy dissipated under four-point flexure and plotted in Figure 5. All of the specimens with hybrid fibers exhibited multiple growths during 0.5 mm to 2.0 mm in the flexural energy absorption, and then, the amount of absorbed flexural energy decreased from 4.0 mm. Among these specimens, the hybrid short PE fiber and SF exhibited higher energy absorption values at all the considered deflection levels. The energy absorption capacity of two w/b values was shown to be similar before 2.0 mm of midspan deflection, and the U17.2 specimens distinctly enhanced the energy absorption capacity to

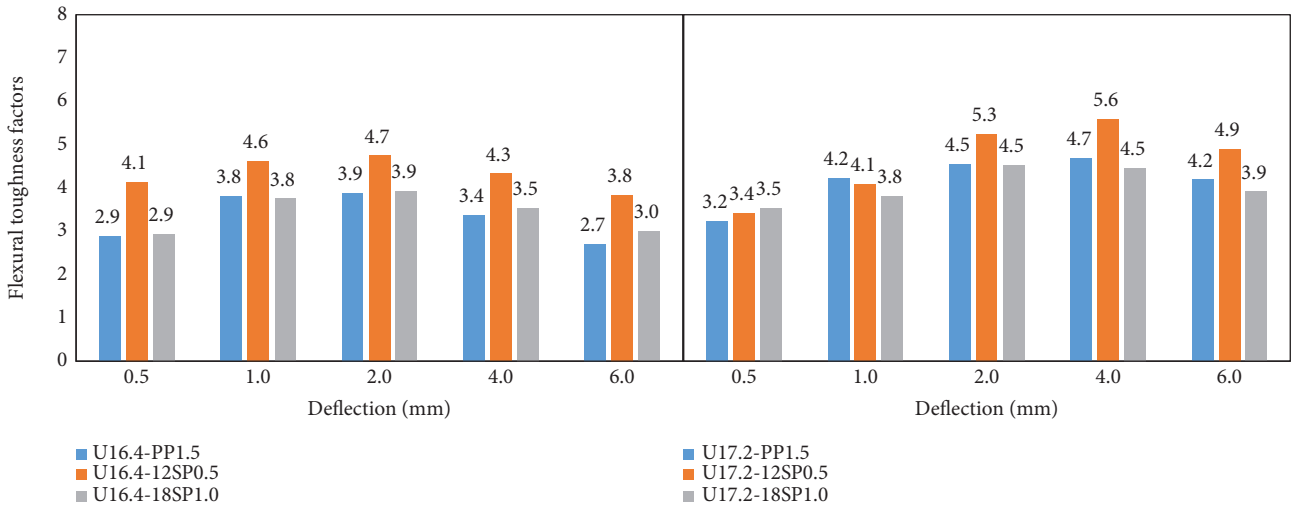

Figure 6: Flexural toughness factors calculated according to the curve in Figure 4 (FT_δ in MPa).

more than that of the U16.4 specimens from 4.0 mm of midspan deflection, as shown in Figure 5. It can be concluded that the different type and different lengths of hybridization fibers can significantly improve the flexural strength, toughness, and energy absorption capacity.

In order to evaluate the synergy in flexure and the effect of fiber hybridization, the flexural toughness factor (FT_δ) was calculated at flexural deflections of 0.5, 1.0, 2.0, 4.0, and 6.0 mm according to equation (1). The behavior was similar to flexural energy absorption, for which the NSHSC hybrid with a short PE fiber and SF exhibited a higher toughening ability at each deflection (Figure 6).

3.3. Synergy in Flexure according to the Various Hybrid Fiber-Reinforced NSHSC. The hybrid fiber-reinforced cementitious composite derives the benefits from each of the single fibers and exhibits a synergetic response [30–33]. Therefore, the various hybrid fibers of NSHSC were evaluated and the synergy was calculated in this study, based on equation (2). Because the materials were nonuniform, a simplistic method was used to evaluate the effect of hybridization on toughness, fracture mechanisms, and the interplay between each fiber within the matrix [33, 34].

$$\text{Synergy} = \frac{FT_{\text{hybrid},a+b}}{(FT_a + FT_b)} - 1, \quad (2)$$

where $FT_{\text{hybrid},a+b}$ denotes the flexural toughness factor to a deflection of various hybridizations and FT_a and FT_b denote the flexural toughness factor to a deflection of individual fiber-reinforced composites.

The method for the synergy analysis was defined based on the concepts of positive synergy, negative synergy, and zero synergy. The positive synergy (synergy > 0) denotes that properties of hybrid fiber-reinforced composite were numerically greater than the sum of the properties produced by the single fiber types, and the negative synergy (synergy < 0) denotes that the properties of the hybrid fiber-reinforced composite were poorer than the sum of the properties produced by the single fiber types, and the zero synergy indicates no synergy in hybridization.

3.3.1. Flexural Behavior of Individual Fiber-Reinforced NSHSC. In order to further evaluate the synergy for the various hybrid fiber-reinforced NSHSCs, specimens with two w/b and a single fiber type (fiber volume fraction according to hybridization) were fabricated and evaluated. The average flexural load-deflection is shown in Figure 7. In the specimens with a fiber volume fraction of 0.5%, NSHSC with SF showed higher postcracking strength and toughness compared with specimens using PE fibers, where the length of the SF was longer than that of the PE fibers. Due to the effect of the PE fiber on multiple-cracking behavior, in the specimens with similar length fibers of 1.0 vol.%, specimens with PE fibers exhibited higher postcracking strength and strain capacity at peak load than those using SF. The flexural behavior of individual fiber-reinforced NSHSC exhibited similar flexural strength to that of fiber hybridization, for which w/b of 17.2% showed more improvement in the properties than a w/b of 16.4% for all of the specimens considered.

3.3.2. Synergy of Hybrid Fiber-Reinforced NSHSC. As previously stated, synergy associated with various NSHSCs has been evaluated. For the striking contrast between specimens hybrid fiber-reinforced and individual fiber-reinforced NSHSCs, the average flexural load-deflection curve by various conditions was shown in Figures 8 and 9, respectively. Furthermore, the synergy of various hybrid fiber-reinforced NSHSCs was calculated and shown in Figure 10.

In the w/b of 16.4%, the specimen hybrid with SF and short PE fibers had positive synergy in all instances (in this study), and the synergy significantly increased with increasing deflection. The toughness of the specimen with 0.5 vol.% exhibited a low value and decreased rapidly from 2.0 mm of deflection, as shown in Figure 8(b). Short PE fibers with low modulus bridged microcracks and improved multicracks in the matrix, whereas long SF arrested the propagation of macrocracks. In contrast, specimen hybrid with

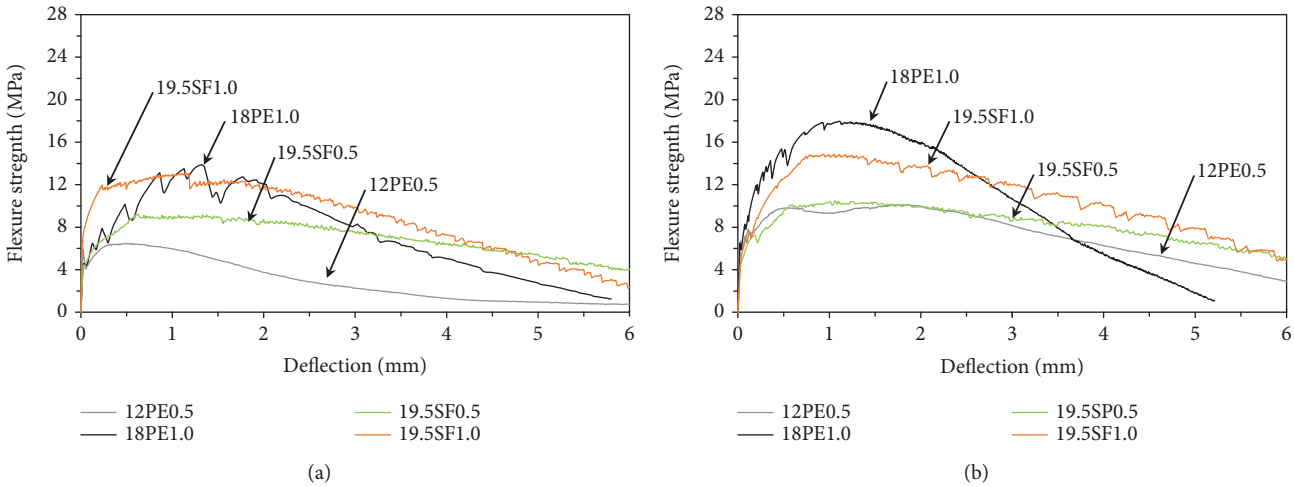

Figure 7: Average flexure load-deflection behavior by individual fibers: (a) various specimens of U16.4 and (b) various specimens of U17.2.

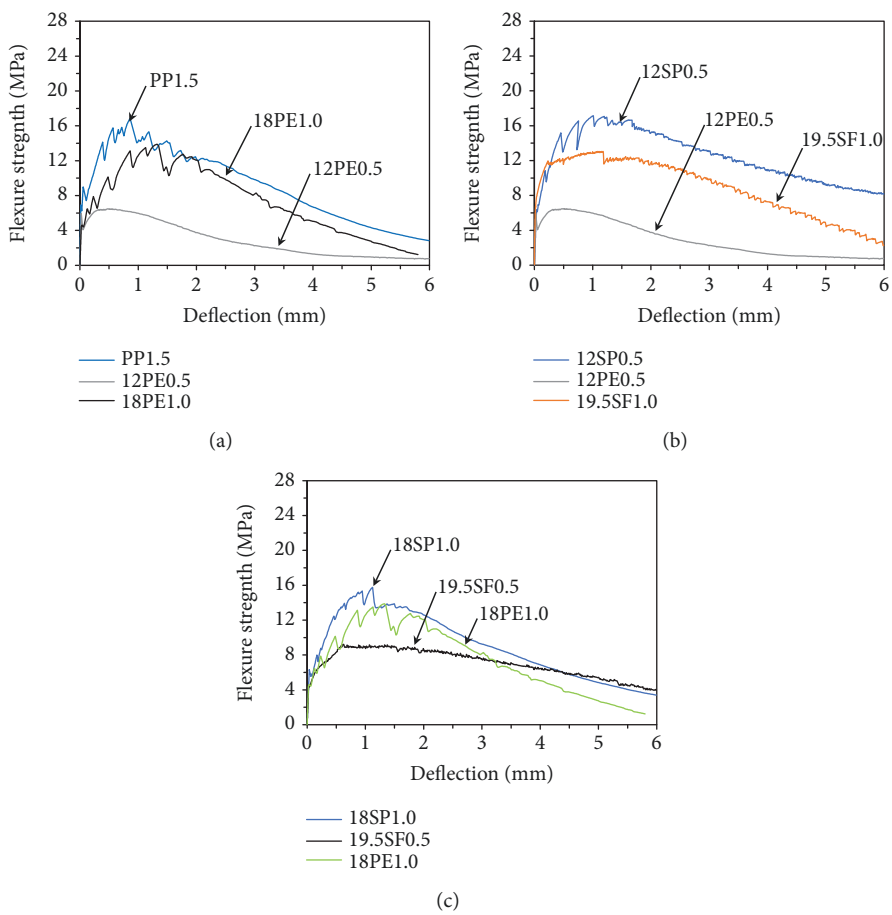

Figure 8: Average flexural load-deflection behavior by various conditions of w/b of 16.4%: (a) U16.4 based on PE fibers with different lengths, (b) U16.4 based on steel fibers with short PE fibers, and (c) U16.4 based on steel fibers with long PE fibers.

different lengths of PE fiber had negative synergy in all cases, and there was almost no variation from 0.5 mm to 6.0 mm. The specimen hybrid with SF and long PE fiber exhibited the negative synergy between 0.5 mm and 4.0 mm, and the synergy gradually approached zero synergy with increasing deflection, before exhibiting positive synergy at 6.0 mm of deflection. Zero synergy occurred in specimens U16.4-12SP0.5 at 0.5 mm of deflection.

In samples with a w/b of 17.2%, there is an indication of the negative synergy before 1.0 mm of deflection in all instances (in this study). The specimen hybrid with SF and short PE fibers indicated positive synergy after 2.0 mm of

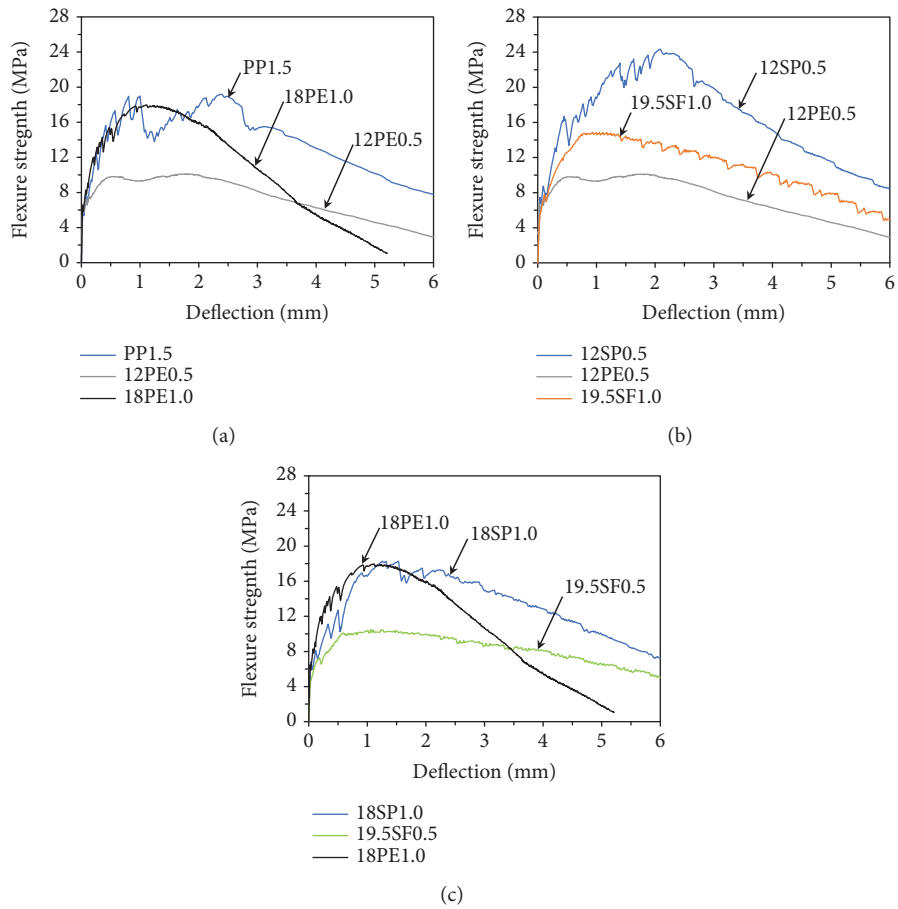

Figure 9: Average flexural load-deflection behavior by various conditions of w/b of 17.2%: (a) U17.2 based on PE fibers with different lengths, (b) U17.2 based on steel fibers with short PE fibers, and (c) U17.2 based on steel fibers with long PE fibers.

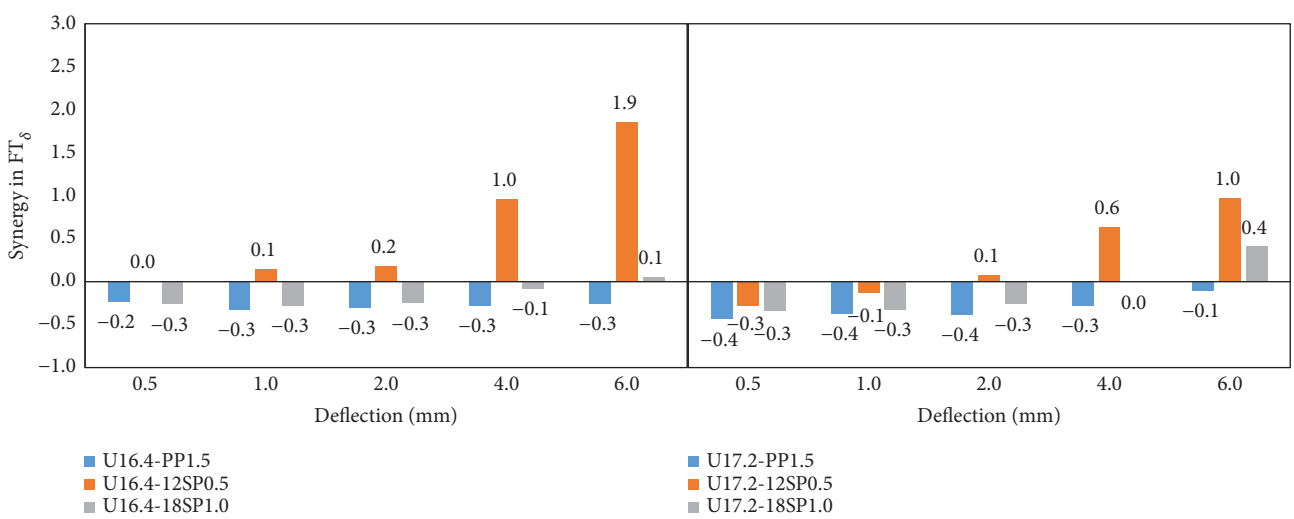

Figure 10: Synergy in flexural properties based on a four-point flexural load-deflection curve.

deflection, and the synergy significantly increased with increasing deflection. The specimen hybrid with steel fiber and long fibers showed positive synergy at 6.0 mm of deflection, and the hybrid with different lengths of PE fiber exhibited negative synergy in all instances, which was a similar behavior to the specimen with a w/b of 16.4%. From the above, the result can be inferred according to the flexural load-deflection curves shown in Figures 8 and 9.

An attempt is made here to identify the hybrid fiber combinations with which NSHSC displayed positive synergy using SF and PE fibers, compared with different lengths of PE fibers based on the flexural toughness. This may be a consequence of hybridizing with PE fibers, whose fiber length and type were weak in the bridging of microcracks. The fiber bridging effect of fiber-reinforced composites was influenced by fiber size (length, diameter), fiber type (modulus), and the bond strength between the fiber and the matrix. However, among those influence factors, the bond strength between the fiber and the matrix should be sufficient to fracture the fiber, which leads to the fiber-reinforced composite exhibiting great ductile behavior. Thus, an increase in the strength of matrix may strengthen the bond between the fiber and the matrix and, in turn, provide increased reinforcement efficiency and toughness. It is possible that, for this reason, NSHSC with SF and PE fiber exhibited better synergy in this study than the hybrid with different lengths of PE fiber-reinforced composite, which had significantly higher compressive strength than the hybrid with different lengths of PE fiber-reinforced composite (Table 5).

4. Conclusions

An experimental investigation was performed to evaluate the mechanical properties of no-slump high-strength concrete with various fiber hybridizations. The three different water-to-binder ratios of various specimens with steel fiber and PE fiber using a fiber volume fraction of 0.0, 1.5% were fabricated and tested compressive strength and under four-point flexure loading at plan age. Furthermore, the flexural toughness and the synergy based on the fiber hybridization were evaluated.

Based on the results of this investigation, the following concluding remarks are obtained:

(1) The specimens with a water-to-binder ratio of 17.2% exhibited a higher compressive strength and low coefficient of variation in all instances. In contrast, the water-to-binder ratio of 16.8% exhibited low properties and not only compressive but also flexural strength, which used 18 mm of polyethylene fibers; hence, it was eliminated at the evaluated mechanical performance of fiber hybridization under study

(2) Flexural strength of hybridization in specimens with fibers had improved over 1.5 times higher postcracking strength than that in specimens without fibers. Due to the PE fibers having low modulus that leads to low strength and high strain capacity and high strength due to high modulus of steel fibers, the specimen hybrid PE fibers with different lengths exhibit a slightly low flexural strength but similar strain capacities (high strain capacities) compared with the specimen hybrid PE fibers and steel fibers. And the water-to-binder ratio of 17.4% of specimens showed a higher flexural strength compare with that of specimens at the same fiber volume fraction

(3) And the exhibited strain hardening based on evaluated toughness, with toughness indices$I_5 > 5$,$I_{10} > 10$, and$I_{30} > 30$, can be defined as a strain-hardening-type composite. However, specimen hybrid with steel fiber and short PE fibers exhibited a higher flexural strength and toughness than that of other various hybridizations, which based on the short fibers that bridge microcracks and control its coalescence to macrocracks; in contrast, the long fibers are aimed at arresting and prohibiting the propagation of macrocracks

(4) A specimen hybrid with steel fiber and short PE fiber indicates positive synergy, and a hybrid with different lengths of PE fiber exhibited the negative synergy in all instances. This may be the consequence of PE fiber length, and the type was weak in the bridged macrocracks due to hybridization with different lengths of PE fibers

Data Availability

The data used to support the findings of this study are available from the corresponding author upon request.

Conflicts of Interest

The authors declare that they have no conflicts of interest.

Acknowledgments

This work was supported by the National Research Foundation of Korea (NRF) grant funded by the Korea government (MEST) (NRF-2016R1A2B3011392).

References

[1] ACI 211.3, *Guide for Selecting Proportions for No-Slump Concrete*, American Concrete Institute, Farmington Hills (MI), 2002.

[2] J. Sobhani, M. Najimi, A. R. Pourkhorshidi, and T. Parhizkar, "Prediction of the compressive strength of no-slump concrete: a comparative study of regression, neural network and ANFIS models," *Construction and Building Materials*, vol. 24, no. 5, pp. 709–718, 2010.

[3] M. Najimi, J. Sobhani, and A. R. Pourkhorshidi, "A comprehensive study on no-slump concrete: from laboratory towards manufactory," *Construction and Building Materials*, vol. 30, pp. 529–536, 2012.

[4] H. Hoornahad, "Toward development of self-compacting no-slump concrete mixtures," Doctoral thesis, Delft University of Technology, 2014.

[5] ACI 207.5, *Roller-Compacted Mass Concrete. American Concrete Institute*, American Concrete Institute, Farmington Hills (MI), 1999.

[6] V. C. Li, "On engineered cementitious composites (ECC): a review of the material and its applications," *Journal of Advanced Concrete Technology*, vol. 1, no. 3, pp. 215–230, 2003.

[7] N. Banthia and R. Gupta, "Hybrid fiber reinforced concrete (HyFRC): fiber synergy in high strength matrices," *Materials and Structures*, vol. 37, no. 10, pp. 707–716, 2004.

[8] S. H. Park, D. J. Kim, G. S. Ryu, and K. T. Koh, "Tensile behavior of ultra high performance hybrid fiber reinforced concrete," *Cement and Concrete Composites*, vol. 34, no. 2, pp. 172–184, 2012.

[9] D. J. Kim, S. H. Park, G. S. Ryu, and K. T. Koh, "Comparative flexural behavior of hybrid ultra high performance fiber reinforced concrete with different macro fibers," *Construction and Building Materials*, vol. 25, no. 11, pp. 4144–4155, 2011.

[10] H. R. Pakravan, M. Latifi, and M. Jamshidi, "Hybrid short fiber reinforcement system in concrete: a review," *Construction and Building Materials*, vol. 142, pp. 280–294, 2017.

[11] N. Banthia and M. Sappakittipakorn, "Toughness enhancement in steel fiber reinforced concrete through fiber hybridization," *Cement and Concrete Research*, vol. 37, no. 9, pp. 1366–1372, 2007.

[12] J. S. Lawler, T. Wilhelm, D. Zampini, and S. P. Shah, "Fracture processes of hybrid fiber-reinforced mortar," *Materials and Structures*, vol. 36, no. 3, pp. 197–208, 2003.

[13] D. L. Nguyen, D. J. Kim, G. S. Ryu, and K. T. Koh, "Size effect on flexural behavior of ultra-high-performance hybrid fiber-reinforced concrete," *Composites Part B: Engineering*, vol. 45, no. 1, pp. 1104–1116, 2013.

[14] S. F. U. Ahmed and H. Mihashi, "Strain hardening behavior of lightweight hybrid polyvinyl alcohol (PVA) fiber reinforced cement composites," *Materials and Structures*, vol. 44, no. 6, pp. 1179–1191, 2011.

[15] P. Richard and M. Cheyrezy, "Composition of reactive powder concretes," *Cement and Concrete Research*, vol. 25, no. 7, pp. 1501–1511, 1995.

[16] ASTM C1437, *Standard Test Method for Flow of Hydraulic Cement Mortar*, ASTM International, West Conshohocken, PA, 2007.

[17] A. Olar, N. Hearn, and D. Wannamaker, "Implementation of the maturity method for zero-slump concrete products," *PCI Journal*, vol. 49, no. 2, pp. 86–97, 2004.

[18] Sørensen and O. Christian, "The stability of fresh zero-slump concrete," *Concrete Research*, vol. 4, no. 3, pp. 656–667, 2013.

[19] ASTM C39/C39M, *Standard Test Method for Compressive Strength of Cylindrical Concrete Specimens*, ASTM International, West Conshohocken, PA, 2014.

[20] ASTM, *C1609/C1609M, Standard Test Method for Flexural Performance of Fiber-Reinforced Concrete (Using Beam with Third-Point Loading)*, ASTM International, West Conshohocken, PA, 2012.

[21] ASTM C1018, *Standard Test Method for Flexural Toughness and First Crack Strength of Fiber Reinforced Concrete (Using Beam with Third-Point Loading)*, ASTM International, West Conshohocken, PA, 1997.

[22] JSCE-G 552-1999, "Test method for bending strength and bending toughness of steel fiber reinforced concrete," in *Standard Specification for Concrete Structures, Test Methods and Specifications*, p. 365, JSCE, 2005.

[23] S. T. Kang, J. I. Choi, K. T. Koh, K. S. Lee, and B. Y. Lee, "Hybrid effects of steel fiber and microfiber on the tensile behavior of ultra-high performance concrete," *Composite Structures*, vol. 145, pp. 37–42, 2016.

[24] A. E. Naaman and H. W. Reinhardt, "Characterization of high-performance fiber reinforced cement composites," in *Proceedings of the Second International RILEM Workshop*, pp. 1–24, USA, June 1995.

[25] K. Q. Yu, J. T. Yu, J. G. Dai, Z. D. Lu, and S. P. Shah, "Development of ultra-high performance engineered cementitious composites using polyethylene (PE) fibers," *Construction and Building Materials*, vol. 158, pp. 217–227, 2018.

[26] S. F. U. Ahmed and M. U. F. Maalej, "Tensile strain hardening behaviour of hybrid steel-polyethylene fibre reinforced cementitious composites," *Construction and Building Materials*, vol. 23, no. 1, pp. 96–106, 2009.

[27] S. F. Ahmed, M. Maalej, and P. Paramasivam, "Analytical model for tensile strain hardening and multiple cracking behavior of hybrid fiber-engineered cementitious composites," *Journal of Materials in Civil Engineering*, vol. 19, no. 7, pp. 527–539, 2007.

[28] I. Markovic, "High-performance hybrid-fiber concrete – development and utilization," Ph. D Thesis T.U.Delft, 2006.

[29] N. Banthia, A. Moncef, K. Chokri, and J. Sheng, "Uniaxial tensile response of microfibre reinforced cement composites," *Materials and Structures*, vol. 28, no. 9, pp. 507–517, 1995.

[30] L. Ferrara, N. Ozyurt, and M. di Prisco, "High mechanical performance of fibre reinforced cementitious composites: the role of "casting-flow induced" fibre orientation," *Materials and Structures*, vol. 44, no. 1, pp. 109–128, 2011.

[31] D. Y. Yoo, N. Banthia, S. T. Kang, and Y. S. Yoon, "Effect of fiber orientation on the rate-dependent flexural behavior of ultra-high-performance fiber-reinforced concrete," *Composite Structures*, vol. 157, no. 6, pp. 62–70, 2016.

[32] N. Banthia and S. M. Soleimani, "Flexural response of hybrid fiber-reinforced cementitious composites," *ACI Materials Journal*, vol. 102, no. 6, pp. 382–389, 2005.

[33] N. Banthia, F. Majdzadeh, J. Wu, and V. Bindiganavile, "Fiber synergy in hybrid fiber reinforced concrete (HyFRC) in flexure and direct shear," *Cement and Concrete Composites*, vol. 48, pp. 91–97, 2014.

[34] Y. W. Mai, R. Andonian, and B. Cotterell, "On polypropylene-cellulose fibre-cement hybrid composites," in *Advances in Composite Materials*, pp. 1687–1699, Proceedings of the Third International Conference on Composite Materials, Pairs, 1980.